Supporting information

Controllable selective exfoliation of high-quality graphene nanosheets and nanodots by ionic liquid assisted grinding

Nai Gui Shang*, Pagona Papakonstantinou*, Shurbhi Sharma†, Genaddy Lubarsky

Nanotechnology and Integrated Bio-Engineering Centre, NIBEC, School of Engineering, University of Ulster, Newtownabbey, BT37 0QB, UK

Meixian Li,

College of Chemistry and Molecular Engineering, Peking University, Beijing, 100871 P.R. China

David W. McNeill

School of Electrical Engineering, Queen's University of Belfast, Belfast, BT9 5AH, UK

Aidan. J. Quinn

Tyndall National Institute, University College Cork, Lee Maltings, Dyke Parade, Cork, Ireland

Wuzong Zhou and Ross Blackley

School of Chemistry, University of St Andrews, St Andrews, KY16 9ST, UK

*corresponding authors: p.papakonstantinou@ulster.ac.uk; ngshang@hotmail.com

† Current address: School of Chemical Engineering, The University of Birmingham Edgbaston, Birmingham B15 2TT, U.K

1. Fabrication process

Graphite powders of 50 mg (99.0% purity, from Sigma-Aldrich) with a grain size less than 20 μm were mixed and ground with 0.1—0.5 mL ionic liquid (IL, 1-Butyl-3-methylimidazolium hexafluorophosphate, $BMIMPF_6$, from Sigma-Aldrich) for 0.5 — 4 hrs. Then the mixtures were added into a solution of 15 mL N,N-dimethylformamide (DMF) and 15 mL acetone and centrifugated in the speed of 3000 rpm for 30 min in order to remove the ionic liquid. This washing cycle was repeated three times and the final sediment was dispersed in 1 L DMF. After one-day sedimentation, the large/thick graphitic flakes completely precipitated on the bottom of the bottle. The supernatant was dried and then the yield was calculated as 20 wt%, which is much larger than that of other methods reported. The supernatant was collected and centrifugated to get a dense suspension, with which the graphene samples were prepared for the study of their microstructure and electrical properties. The suspension was diluted and dropped on lacy carbon-coated Cu grid for TEM observations, on clean Si wafers or mica sheets for the XPS, Raman and AFM studies, and on thermally oxidised Si wafer substrates (300 nm SiO_2) for the study of electrical properties. Note, to obtain uniform large-area graphene thin films, the Si/SiO_2 substrate was functionalised with 5% 3-triethoxysilylpropylamine (APTES) aqueous solution for 30 min. All samples were completely dried under an infrared light or on a hot plate before measurements.

We should note the role of ILs in this study. ILs are low-temperature molten salts, and as their name denotes are liquids composed entirely of ions. They have been proposed as a new class of “green” organic solvents because not only they are able to solvate a large variety of organic and inorganic compounds, (polar or non-polar) but also they possess high thermal and chemical stability, high ionic conductivity, wide electrochemical window, and negligible vapour pressure. The mixing of a small quantity of IL and graphite flakes forms a gel-like composite. When graphite flakes are ground with ionic liquids, the shear force detaches the graphene layers from the graphite flakes. The ionic liquids can effectively surround each layer preventing the detached graphenes from restacking. Based on simulation and experimental studies on processing of carbon nanotubes with imidazolium-based ILs, the electronic structure of graphene layers in the bucky gel remains unchanged and there is no charge transfer between graphene and imidazolium cations[1].

2. XPS data analysis

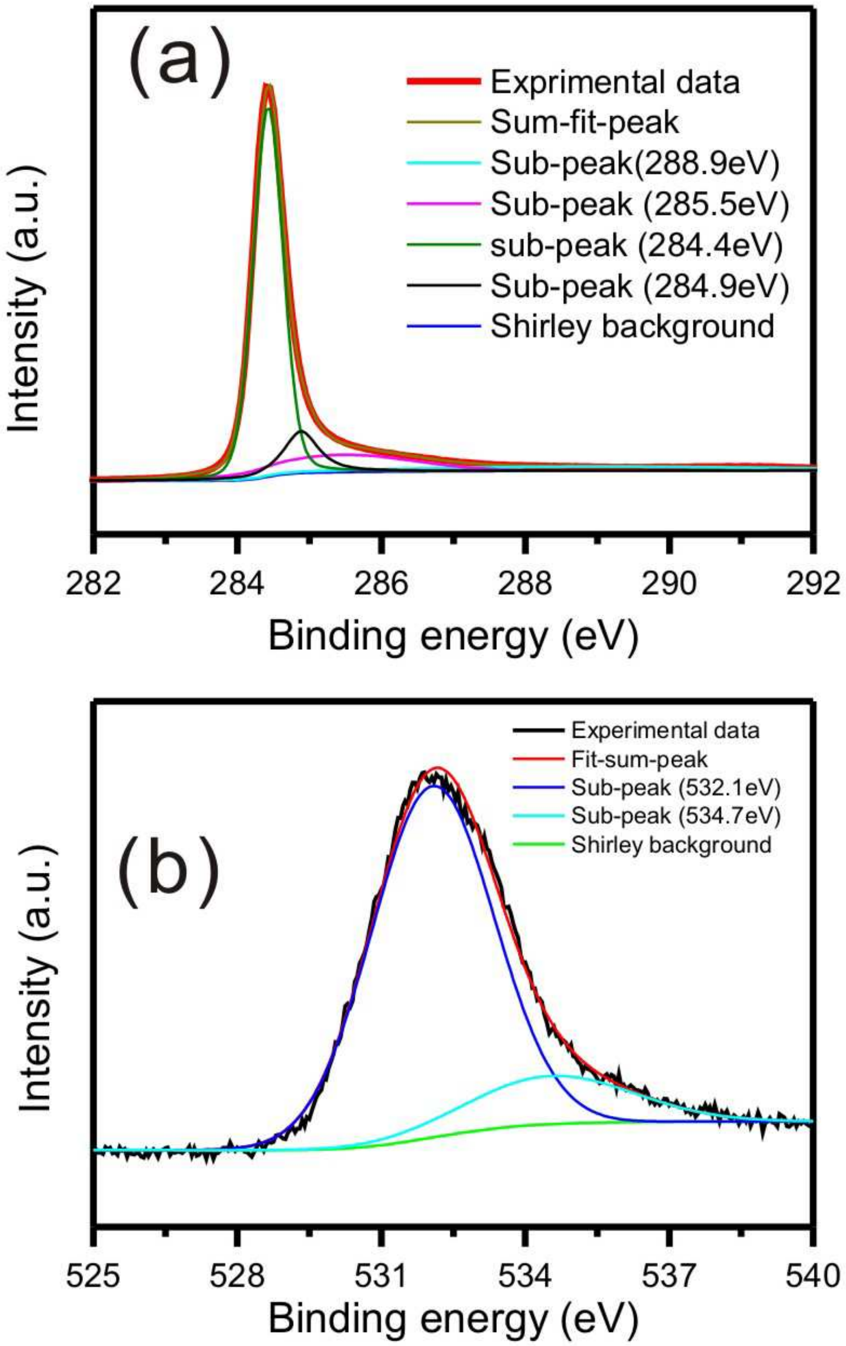

Figure S1. XPS narrow scan spectra of graphene samples for elements C 1s (a) and O1s (b), respectively.

Figure S1 (a) and (b) present a high resolution asymmetric C1s and an O1s XPS spectrum of graphene sheets, respectively. After subtraction of a Shirley background followed by a fitting process using a mixture of Lorentzian and Gaussian lineshapes, the C1s peak was deconvoluted into four sub-peaks located at 284.4, 284.9, 285.5, and 288.9 eV, which have been assigned to C-C (sp^2), “defect peak”, C-O and COOC/COOH bonds, respectively. The O1s peak can be fitted by two Gaussian peaks at 532.1 and 534.7 eV corresponding to C-O and C=O bonds.

3. Low magnification TEM images of graphene nanosheets and their size distributions

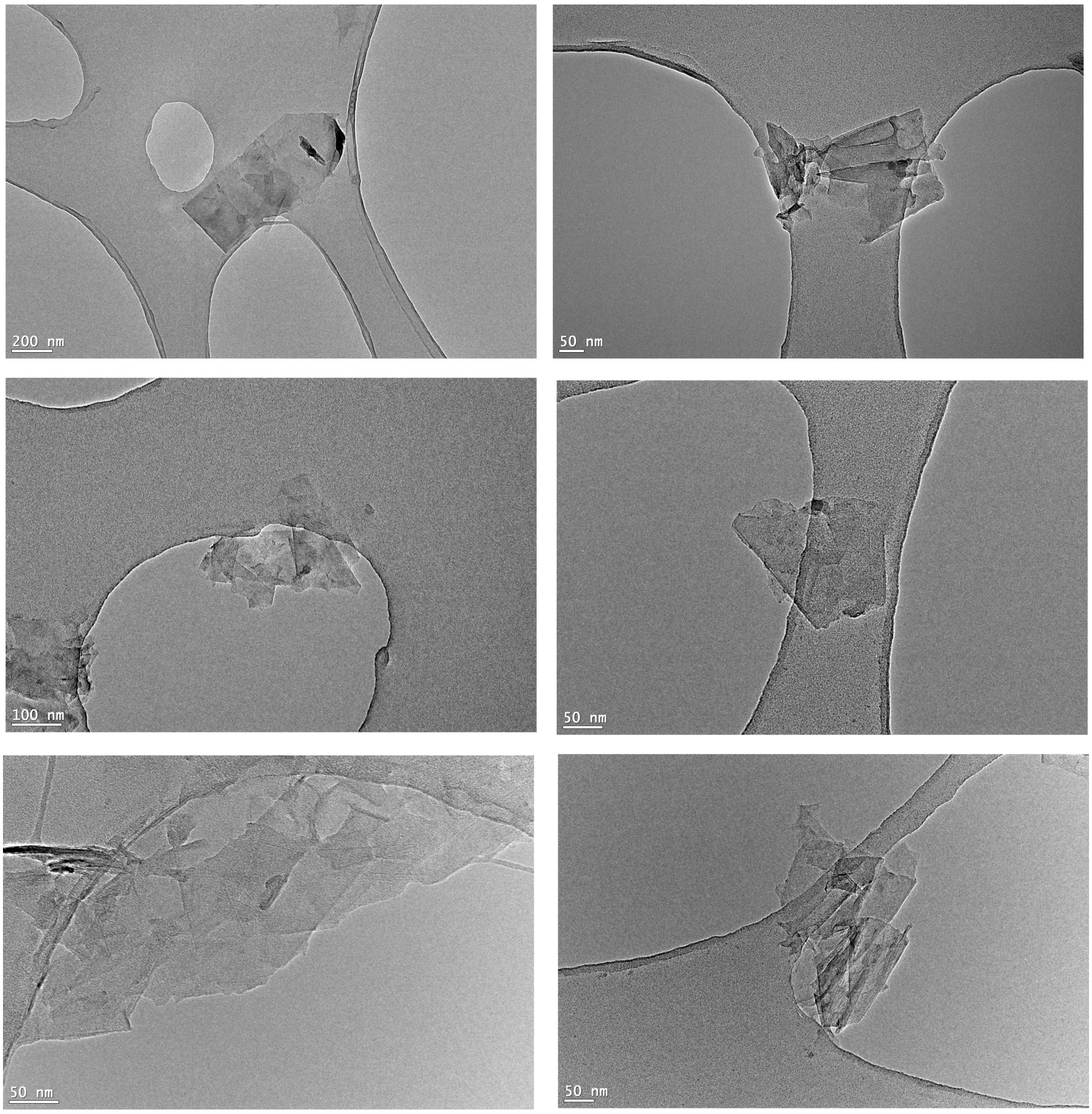

Figure S2. Low magnification TEM images of folded and wrinkled graphene nanosheets.

4. Size distribution of graphene nanodots

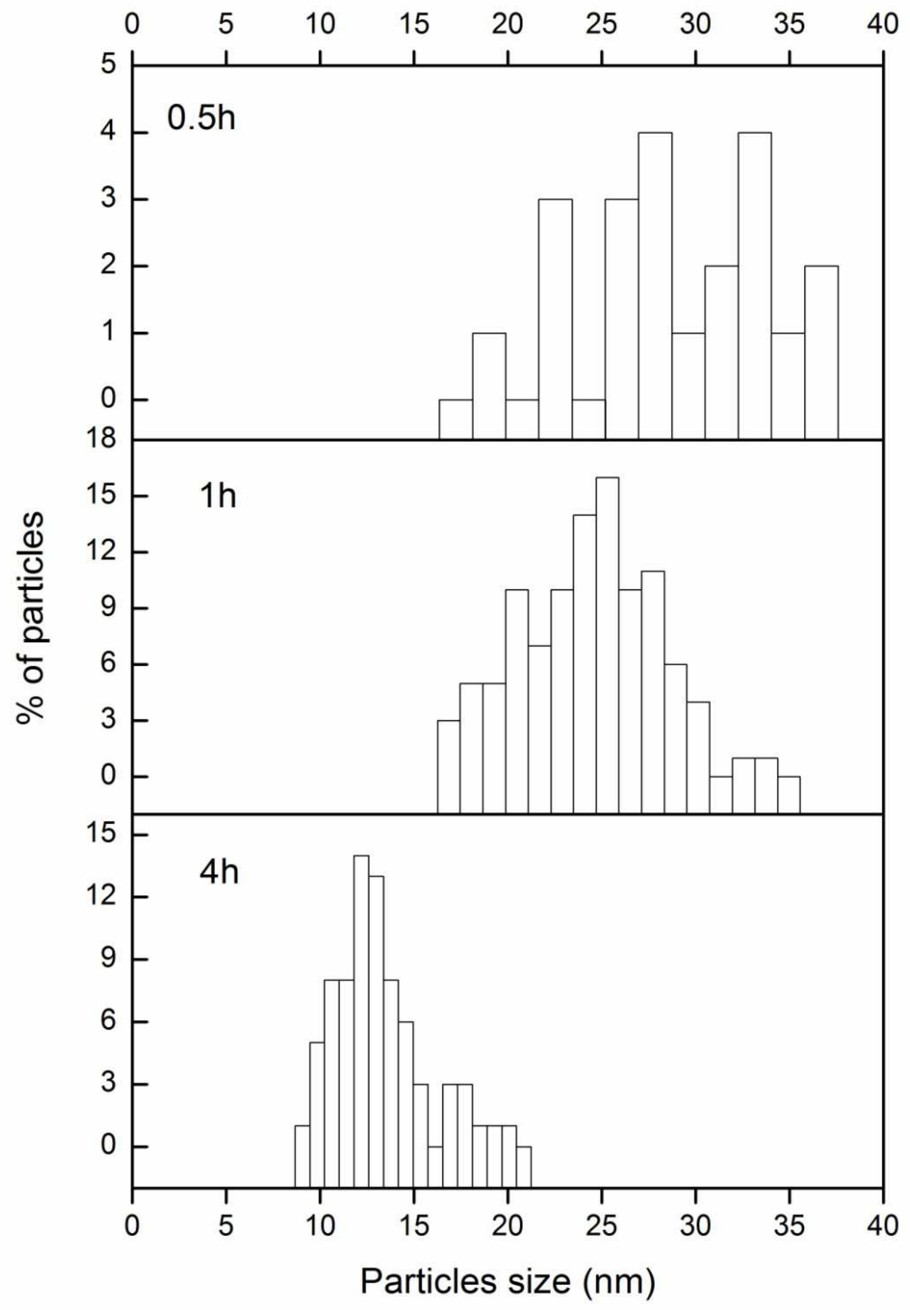

Figure S3. Histogram of graphene nanodots describing their size distribution.

5. AFM images and profile line scans of graphene nanodots

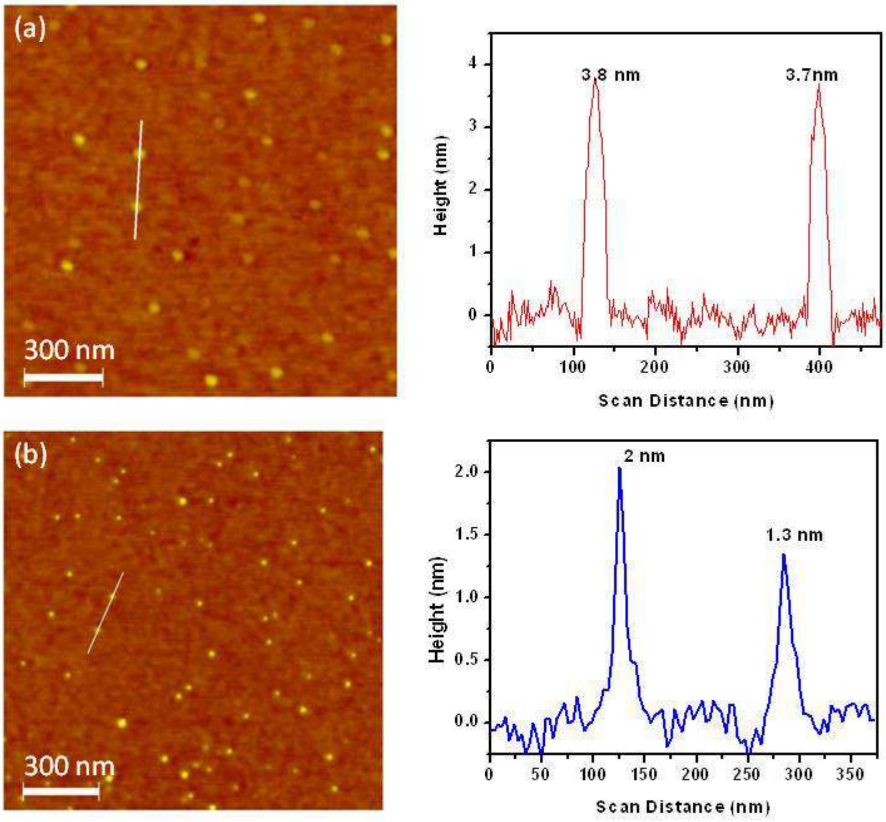

Figure S4. Typical Atomic Force Microscopy images and topography line profiles for graphene nanodots produced using different grinding times: (a) 1 hour, (b) 4 hours .

6. SEM images of graphene nanosheets

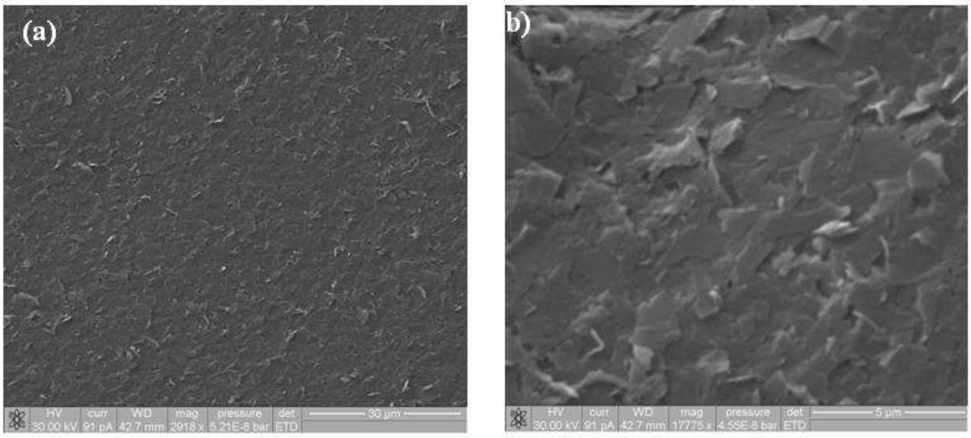

Figure S5. Different magnification SEM images of graphene sheet films produced through filtration of graphene solution.

7. Raman spectrum of graphene sheets and nanodots

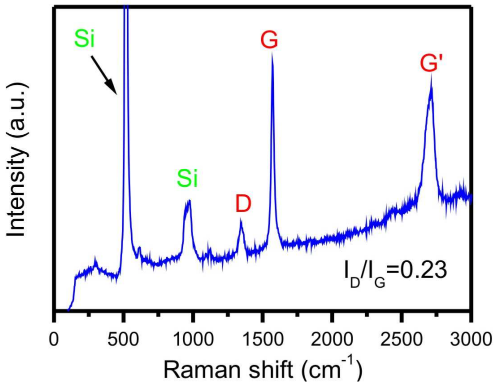

Figure S6. Typical Raman spectrum of the graphene nanosheets.

Raman scattering is a convenient, powerful macroscopic tool for the characterisation of graphene. The layer number and quality of graphene fabricated by the method of micromechanical cleavage can be well distinguished by the analysis of spectroscopic intensity, frequency and line width etc. Figure S6 shows a typical Raman spectrum of the graphene sample. The Raman measurement is conducted in a backscattering geometry at room temperature using an excitation laser of 514 nm with a spot size of 1-2 μm. There are three strong peaks at 1348, 1571, and 2711 cm^{-1}, which are ascribed to the D, G, and G´ bands of graphitic materials, respectively. No broad peaks relevant to amorphous carbon are found in the sample. The presence of the D peak arises from the edges of graphene sheets, whoose size is smaller than the laser spot (1-2μm). The ratio of integrated intensities of D to G bands (I_D/I_G) is only 0.23, revealing that the graphenes we produced are of high quality, since the D band is a fingerprint of defects in graphitic materials. The G´ band, a fingerprint of graphene, is quite strong, larger than the D but slightly smaller than the G band in intensity. The ratio of integrated intensity of G´ to G bands is about 0.61, revealing the presence of 2-4 graphene layers consistent with the TEM observation. Note, currently the Raman spectra of graphene fabricated by solution based methods do not resemble those of graphene produced by other methods. They do not present identical spectroscopic features and are strongly dependent on the fabrication method and chemicals used. Most of them present a strong D band, a broad G band and a weak G´ band. However, all findings presented here confirm that the crystalline quality of graphene we produced is better to those reported by solution methods in other groups, but poorer than the graphene produced by mechanical cleavage of highly oriented pyrolytic graphite and by high-temperature CVD growth on metal substrates, where no defect related D bands can be detected. The relatively poorer quality of graphene sheets is believed to be due to the low-quality starting material (natural graphite) compared to the HOPG, and not due to the grinding process.

8. TGA spectra of the starting graphite and produced graphene

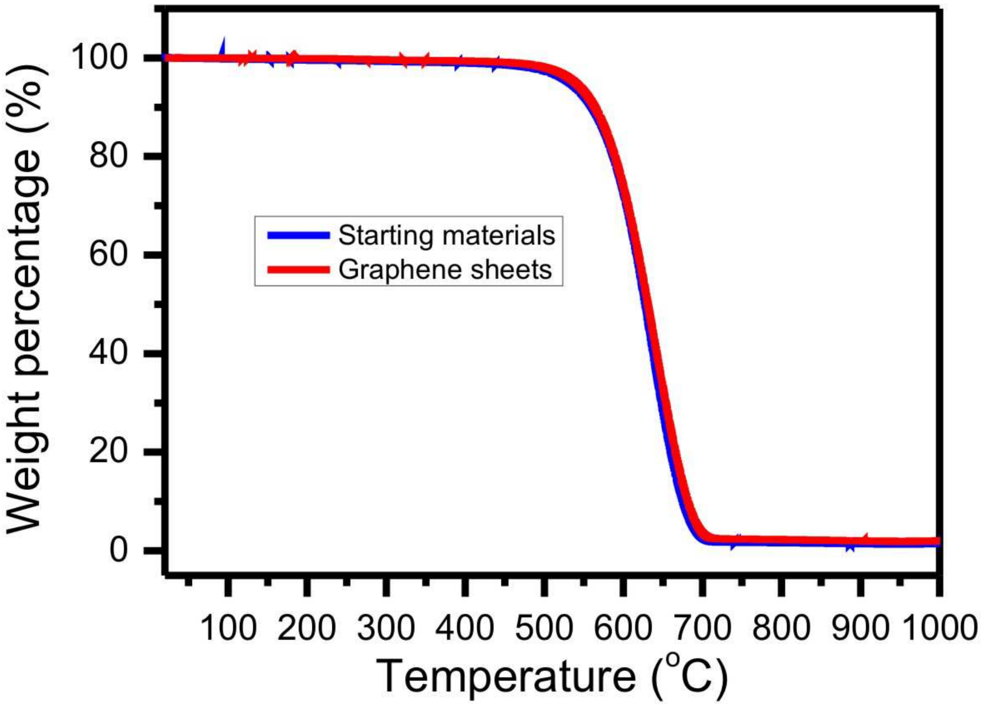

Figure S7. TGA spectra of graphene sheets and starting graphite flakes material.

Figure S7 shows TGA spectra taken from the graphene sheets and the starting graphite flakes material. The measurement was done in a mixture ambient of 50 % N_2 and 50 % O_2 with a ramp of 1 ºC/min. It can be seen that graphene sheets have a same thermal behaviour as that of the starting material. They simultaneously start to oxidize at around 500 ºC and completely burn off at 700 ºC, demonstrating exactly same quality and no any high/low melting materials being introduced in the fabrication process.

9. Electrical resistivity of pristine and vacuum-annealed graphene nanosheet films

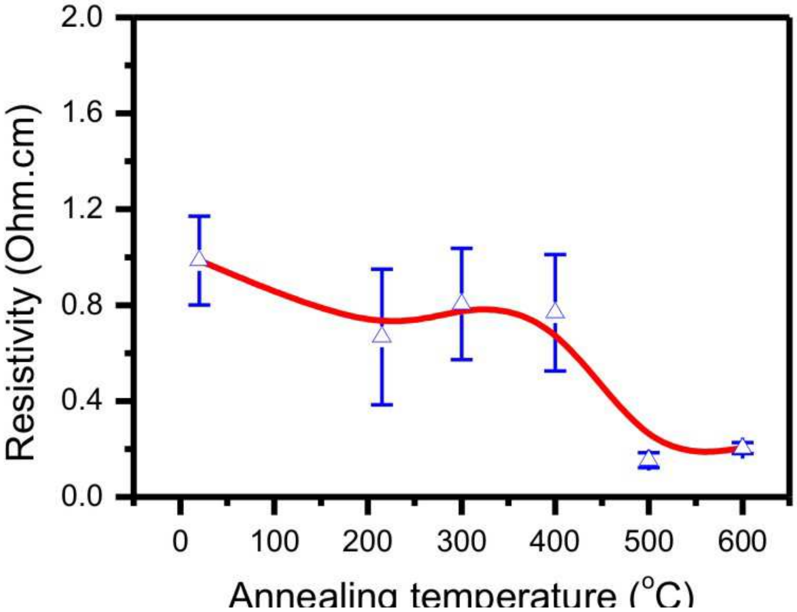

Figure S8. The resistivity of graphene sheet films as a function of the annealing temperature.

Figure S8 shows the resistivity of graphene films as a function of the annealing temperature. The graphene films with a thickness of around 12.8μm were fabricated on a large SiO_2 coated Si wafer by drop coating and then were cut into several 10×20 mm^2 sized pieces for annealing in vacuum (less than 8×10^{-5} Torr) for 1 hr in the temperature range of 200 – 600 ºC. The resistances were measured by a four-probe technique at room temperature (Resistivity test rig, Model B, A & M Fell LTD, England). The resistivity of pristine graphene films is about $1\times10^{-2}\Omega\cdot m$. The resistivity decreases to $8\times10^{-3}\Omega\cdot m$ with the increase of the annealing temperature in the range of 200 – 400 ºC. When the annealing temperature is increased to 500 – 600 ºC, their resistivity significantly lowers to $2\times10^{-3}\Omega\cdot m$. However, this value is still larger than that ($0.07 - 0.11\times10^{-3}\Omega\cdot m$) of graphene films produced by other chemical solution methods.[2] The main reason is that there are a lot of junctions in the film due to either the smaller size of single graphene sheets or the presence of voids. The standard deviations of pristine and annealed graphene films at low temperatures are quite large, suggesting that the graphene film could have different thicknesses and different numbers of internal structural voids. The variation of the graphene resistivity appears to take place in two steps, suggesting that the graphene film is subjected to two kinds of transitions during annealing. The first process could be due to the desorption of various absorbates such as water, C-H and COOH groups from the surface of graphene films and the inner surface of the structural voids. The second step could be ascribed to the shrinking or collapsing of the voids, leading to relocation of all constituent graphene sheets and the formation of a dense uniform film at high temperature, which is evidenced by the small value of standard deviation in the resistivity data at this temperature.

TEM images of graphene nanodots

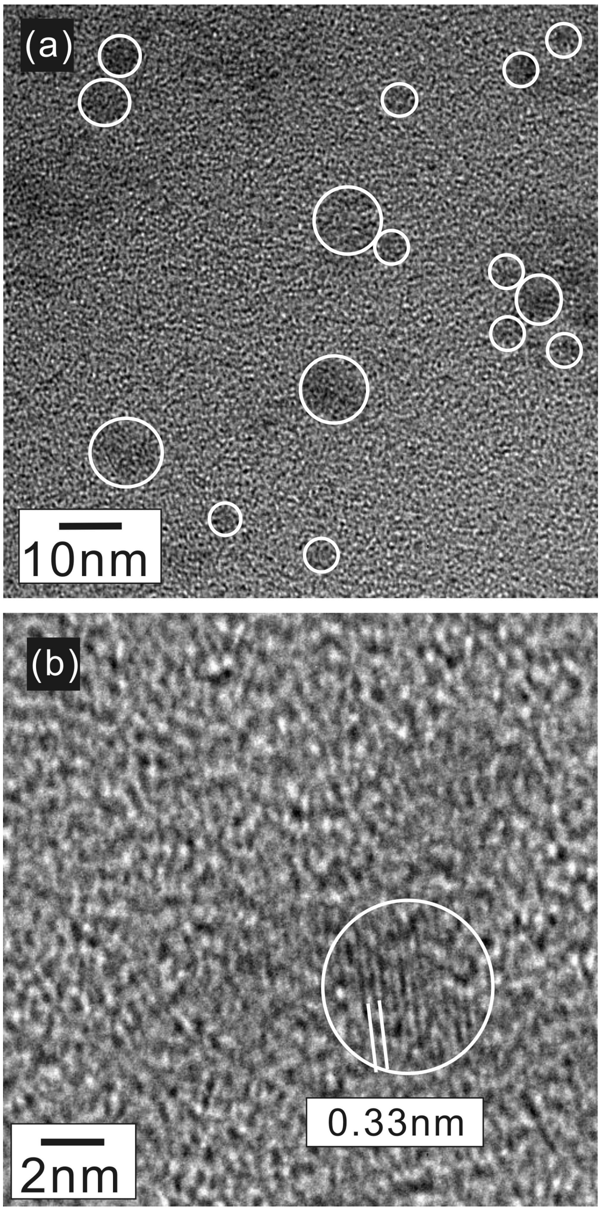

Figure S9. Typical TEM images of graphene nanodots.

Figure S9(a) shows a typical low-magnification TEM images of graphene nanodots which are produced by grinding for 4hrs. The graphene nanodots have a size of 5-12 nm, in close agreement with the AFM results. The high-resolution TEM image (Fig. S9b) shows the high crystalline quality of nanodots with a lattice spacing of around 0.33nm.

10. Optical properties of graphene nanodots

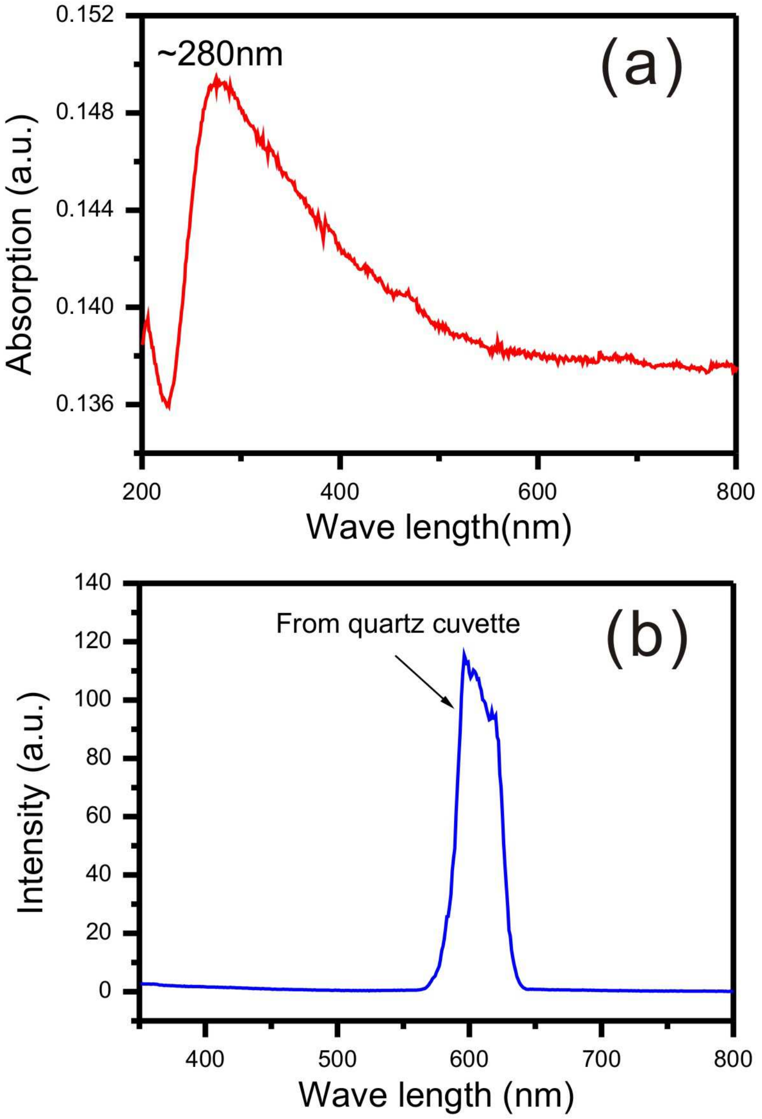

Figure S10. (a) UV-Vis absorption and photoluminescence spectra of graphene nanodots.

Figure S10 (a) shows a typical UV-Vis absorption spectrum taken from ~0.1mg/mL graphene nanodots in de-ionized water by using a UV-Vis spectrometer (Perkin Elmer Lambda 35). The graphene nanodots have a broad absorption band centered at around 280nm. Figure S10 (b) shows a typical photoluminescence spectrum taken from ~0.03mg/mL graphene in DMF solution using a Cary Eclipse fluorescence meter with a 330 nm filtered excitation at room temperature in a wavelength range of 350-800nm. It can be seen that there is a strong broad red band centered at 610 nm, which originates from the quartz cuvette rather than from the graphene nanodots. No photoluminescence from the graphene nanodots was observed. This was confirmed by a control experiment with a bare DMF solution. The main reason for the absence of PL in the graphene nanodots produced by IL assisted grinding in the present work is that they are free of both the defects and functional groups, which are usually considered to result in PL.[3] [4]

References:

---

[1] J. Wang, H. Chu and Y Li, *ACS Nano*, 2008, **2**, 2540–2546.

[2] S. De and J. N. Coleman, *ACS Nano*, 2010, **4,** 2713-2720.

[3] N. G. Shang, U. Vetter, I. Gerhards, H. Hofsass, C. Ronning and M. Seibt, *Nanotechnology*, 2006, **17**, 3215-3218.

[4] S. N. Baker and G. A. Baker, *Angwe. Chem. Int. Ed.* 2010, **49**, 2-21.

.